EUKARYOTIC CELL, Apr. 2011, p. 604–610 Vol. 10, No. 4
1535-9778/11/$12.00 doi:10.1128/EC.00296-10

Role of B Regulatory Subunits of Protein Phosphatase Type 2A in Myosin II Assembly Control in *Dictyostelium discoideum*▽†

Vandana Rai and Thomas T. Egelhoff*

Department of Cell Biology, Lerner Research Institute (NC10), The Cleveland Clinic Foundation, 9500 Euclid Avenue, Cleveland, Ohio 44195

Received 29 November 2010/Accepted 16 February 2011

In *Dictyostelium discoideum*, myosin II resides predominantly in a soluble pool as the result of phosphorylation of the myosin heavy chain (MHC), and dephosphorylation of the MHC is required for myosin II filament assembly, recruitment to the cytoskeleton, and force production. Protein phosphatase type 2A (PP2A) was identified in earlier studies in *Dictyostelium* as a key biochemical activity that can drive MHC dephosphorylation. We report here gene targeting and cell biological studies addressing the roles of candidate PP2A B regulatory subunits (phr2aBα and phr2aBβ) in myosin II assembly control *in vivo*. *Dictyostelium* phr2aBα- and phr2aBβ-null cells show delayed development, reduction in the assembly of myosin II in cytoskeletal ghost assays, and defects in cytokinesis when grown in suspension compared to parental cell lines. These results demonstrate that the PP2A B subunits phr2aBα and phr2aBβ contribute to myosin II assembly control *in vivo*, with phr2aBα having the predominant role facilitating MHC dephosphorylation to facilitate filament assembly.

Myosin II plays critical roles in cytokinesis, cortical tension maintenance, cell migration, and multicellular development in *Dictyostelium discoideum* cells. *In vivo* myosin II function requires assembly into bipolar filaments, allowing interaction with cortical actin and force production. In resting *Dictyostelium* cells, a majority of the cell's myosin II resides in a soluble cytosolic pool, which is rapidly assembled into cytoskeletal bipolar filaments during cell motility in response to chemotactic stimuli (1). Phosphorylation of three threonine residues at positions 1823, 1833, and 2029 of the MHC regulates filament assembly and localization of myosin, with phosphorylation driving filament disassembly (5, 7). Dephosphorylation is necessary for filament assembly *in vitro* and *in vivo*, and exchange between the assembled and soluble pools in live cells is remarkably rapid, with a half-life ($t_{1/2}$) of ~7 s in live cells (22, 23). A series of three MHC kinases (MHCK A, MHCK B, and MHCK C) were identified in previous work and were demonstrated to mediate filament disassembly in live cells (13, 23).

Although the MHCKs that mediate *in vivo* assembly control have been established, protein phosphatases involved in assembly control have not been well studied. Murphy and Egelhoff reported PP2A as a major MHC phosphatase in *Dictyostelium* in studies using purified myosin II and biochemical fractionation approaches (16). In those studies, PP2A holoenzyme displayed substantially higher activity toward myosin phosphorylated on the heavy chains than it did toward myosin phosphorylated on the regulatory light chains (RLC), supporting the hypothesis that PP2A may have a physiological role in the control of filament assembly (16).

The heterotrimeric PP2A holoenzyme is a highly conserved regulatory system in diverse eukaryotes. The core PP2A consists of an ~36-kDa catalytic subunit (pho2A) tightly associated with a 65-kDa scaffolding A subunit (pppA), forming an AC dimer which then associates with one of the many variable "B-type" subunits, such as B, B′, B″, and B‴, encoded by separate genes (11). B subunits of PP2A function in targeting the phosphatase activity to specific substrates or specific subcellular locations, thereby conferring specificity to the enzyme (10). A role for the 55-kDa B subunit in cell cycle control has been demonstrated in *Drosophila* based upon the mitotic defects observed in B-subunit mutants (15). Recent studies resolving the structure of the PP2A/B56 holoenzyme indicate that the carboxyl side of B56 could partially block the active site of the PP2A catalytic subunit P2Ac (3, 21). Likewise, other regulatory subunits could also affect the phosphatase activity, either positively or negatively, in addition to their roles of substrate interaction and subcellular localization of the PP2A holoenzyme (14). In this study, we described the role of the PP2A regulatory subunit in myosin II assembly in *Dictyostelium*.

Dictyostelium genome analysis reveals five candidate variable subunits, two being possible B-type subunits. The first of these, here designated B55α (phr2aBα), was originally identified via mass spectroscopy and Western blotting as a subunit of the biochemically isolated trimeric MHC phosphatase described previously (16, 17). In the current work, we describe the consequences of gene disruption of phr2aBα and consequences of gene disruption of a closely related gene in the *Dictyostelium* genome that has been annotated phr2aBβ. This analysis supports a role for phr2aBα in enhancing PP2A core activity toward myosin II and suggests that phr2aBβ has a more minor role in helping target PP2A activity toward myosin II.

* Corresponding author. Mailing address: Department of Cell Biology, Lerner Research Institute (NC10), The Cleveland Clinic Foundation, 9500 Euclid Ave., Cleveland, OH 44195. Phone: (216) 445-9912. Fax: (216) 444-9404. E-mail: egelhot@ccf.org.

† Supplemental material for this article may be found at http://ec.asm.org/.

▽ Published ahead of print on 25 February 2011.

MATERIALS AND METHODS

Cell culture. The *Dictyostelium discoideum* cell line AX2 was used as the parental line for all experiments. Cells were grown at 21°C in HL5 growth medium supplemented with penicillin-streptomycin (100 U/ml) on petri plates. Medium was supplemented with 2 μg/ml blasticidin for knockout selection.

Gene disruption. The phr2aBα and phr2aBβ knockout cell lines were generated via disruption of the phr2aBα and phr2aBβ loci in the AX2 parental line. Disruptions were generated using a blasticidin-resistance cassette, and the resultant blasticidin-resistant colonies were screened via PCR for the disruption of genes to identify knockout clones. Candidate phr2aBα knockout clones were further confirmed by Western blot analysis. Disruption of the phr2aBα gene was performed as follows. A short 5′ segment of the phr2aBα gene, 673 bp in length, was PCR amplified from AX2 genomic DNA using primer B55α634-EcoRI (P1; GCGCGA ATTCGCGTAATAATACTGCTATTGTCGTC) and primer B55α1307-BamHI (P2; GCCGGGATCCCGCCGGGATCCCCAGTTTGGTCAAACTCTATAGC). This fragment was subcloned into EcoRI-BamHI-digested pBsr-Nsi plasmid vector (2) to generate pBsr-Nsi-phr2aB55α-Ex1-2vector. Similarly, a 3′ segment of the phr2aBα gene, 707 bp in length, was PCR amplified using primer B55α2515-HindIII (P3; GCGCAAGCTTGTAGATATTAAACCAACCAACATGG) and primer B55α222-EcoRI-HindIII (P4; GGCCAAGCTTGAATTCAGTAGCAGCATATA AATACACGG). This fragment was subcloned into pBsr-Nsi-phr2aB55α-Ex1-2vector to create the knockout vector pBsr-Nsi-phr2aB55α. From this vector DNA, the entire knockout cassette carrying a blasticidin resistance cartridge in the middle was excised with EcoRI and HindIII, purified, and used for electroporation of AX2 cells. Transformants were selected in the presence of 2 μg/ml blasticidin in the growth medium. Individual clones were isolated, amplified, and subjected to further analyses using primers. The phr2aBβ knockout was generated by PCR amplification of a 5′ gene fragment of a 849-bp pair using primer B55β1030-EcoRI (P5; GCGC GAATTCAGAATTACATCCAAATGGTG) and primer B55β1879-BamHI (P6; CGCGGATCCTTGCGCTGCCATTTAAACTT) and subcloned into vector pBSR-Nsi to generate pBsr-Nsi-phr2aB55α-Ex-1vector. Next, a 3′ gene fragment of 648 bp was amplified by PCR using primer B55β2389-HindIII (P7; GCGCAAGC TTGATATGTCATTTTCATTGGATGG) and primer B55β3073EcoR-HindIII (P8; GGCCAAGCTTGAATTCTGTTGAAATTGAGCCAATCCT). The purified fragment was cloned in pBsr-Nsi-phr2aB55α-Ex1-2vector to create the knockout vector pBsr-Nsi-phr2aB55β. Electroporation and colony selection were performed as described above.

Western blot analysis. Total cell lysates for the Western blot analyses were generated by collecting 1×10^7 cells growing on 10-cm plates by centrifugation at $350 \times g$ for 5 min at 4°C. Cells were washed twice with the ice-cold 50 mM TES [*N*-tris(hydroxymethyl)methyl-2-aminoethanesulfonic acid] buffer, pH 7, and then resuspended in 50 mM TES buffer containing protease inhibitor cocktails PIC1 and PIC2 (20). An equal volume of prewarmed sample buffer carrying 1 mM 2-mercaptoethanol was added and boiled at 95°C for 1 min. Lysate samples (10 μl) were subjected to electrophoresis on 4% to 20% SDS-acrylamide gel. Following SDS-PAGE, the gels were transferred to a polyvinylidene difluoride membrane using a Trans-Blot SD semidry transfer cell and probed with each primary antibody in Tris-buffered saline (TBS) containing 2.5% milk, 0.1% Tween 20 overnight at 4°C. After incubation with the primary antibodies, the blots were washed in TBS containing 0.1% Tween and then probed with either monoclonal mouse or polyclonal rabbit antiserum diluted in TBS, 0.1% Tween. The blots were detected with a chemiluminescence detection system. Antibodies used in this study include a commercial polyclonal antibody that recognizes the carboxyl terminal of the PP2A C subunit (no. 2038; Cell Signaling, Inc.); a previously described anti-phr2aBα peptide antibody and anti-pppA fusion protein antibody (16); an anti-myosin II monoclonal antibody, My4 (18); and an anti-actin (A2066; Sigma).

Development and phototaxis assay. Cells (1×10^7) were collected and developed on starvation buffer-agar plates, and images were taken after 24 h, 48 h, and 72 h of development. For the phototaxis assay, parental and null cells (1×10^7) were concentrated in 100 μl starvation buffer and plated in ~10-mm spots on agar plates made with starvation buffer. Cells were allowed to migrate toward the pinhole light source for 48 h on the plate covered with aluminum foil. Images were taken after 48 h (8).

Suspension growth analysis. Cells were cultured in suspension with a reciprocal shaker at 160 rpm, and the cell population was counted by a hemocytometer every 24 h for 7 days.

Counting of nuclei. Cells growing in suspension culture or on plastic petri plates for 72 h were collected and seeded in glass-bottomed microscope chambers to examine the number of nuclei. Chambers were kept at room temperature for 20 min to settle cells, and then growth medium was removed and cells were fixed with 4% formaldehyde in 15 mM phosphate buffer, pH 6.2. Cell nuclei were stained by adding 1 ml freshly diluted 4,6-diamidino-2-phenylindole (DAPI) solution (20 μg/ml) and incubated for 5 min at room temperature. DAPI solution was removed, followed by washing cells twice with phosphate-buffered saline (PBS) at room temperature. After 1 ml PBS was added, cells were visualized by an inverted light microscope for stained nuclei.

Triton-insoluble cytoskeleton fractions. Assembled myosin II filaments cofractionate with Triton X-100-resistant cytoskeletal ghosts when *Dictyostelium* cells are lysed under mild conditions. Cells (2×10^6) were washed in starvation buffer (20 mM MES [morpholineethanesulfonic acid], pH 6.8, 0.2 mM $CaCl_2$, 2 mM $MgCl_2$), then resuspended in 150 μl of ice-cold buffer A (0.1 M MES, pH 6.8, 2.5 mM EGTA, 5 mM $MgCl_2$, 0.5 mM ATP) and chilled on ice. Samples were then mixed with 150 μl buffer B (same as buffer A but also contains 1% Triton X-100 and protease cocktail mix PIC1 and PIC2). Samples were vortexed at top speed for 5 s and then subjected to centrifugation in a microcentrifuge at top speed at 4°C for 2 min. Pellets (cytoskeletal fractions) were directly suspended in sample buffer and heated at 95°C for 60 s. Supernatants (cytosolic fractions) were precipitated with 700 μl acetone with incubation on ice, followed by centrifugation for 10 min to collect protein. Dried supernatant protein pellets were then suspended in sample buffer and heated. Samples were subjected to SDS-PAGE, and the percentage of myosin II in the cytoskeleton was calculated for each individual sample by dividing the densitometry value for the myosin heavy chain in the cytoskeletal pellet by the sum of the pellet and supernatant myosin heavy chain values for that sample and multiplying this value by 100.

RESULTS

Elevated PP2A subunit RNA expression during active chemotactic cell migration phase. As one measure of possible PP2A involvement in myosin II heavy chain dephosphorylation *in vivo*, we queried the online *Dictyostelium* RNASeq database (19) to see if myosin II, myosin II heavy chain kinases, and PP2A expression rise during the active chemotactic phase of *Dictyostelium* development. Scaled read counts revealed strong induction of both myosin II heavy chain (*mhcA*) and myosin II regulatory light chain (*mlcR*) expression during the active chemotactic phase (see Fig. S1 in the supplemental material). The established MHC kinases MHCK A, B, and C also displayed increases in expression through the same period of development (see Fig. S1B), with MHCK A and B displaying the greatest induction. Analysis of protein phosphatase gene expression revealed strong induction of PP2A core dimer subunits pho2a and pppA and of the phr2aBα subunit that was originally identified in the work of Murphy and Egelhoff (16). Although the related phr2aBβ showed increases in scaled sequence reads at 4 h of development, overall expression of phr2aBβ was very low relative to that of other PP2A subunits (see Fig. S1C). In contrast to the sharp induction of PP2A subunits by 4 h of development, the catalytic subunit of PP1 (pppB) displayed the strongest induction at 8 to 24 h (see Fig. S1C). Given the established peak of actomyosin-based cell migration at the ~4- to 8-h window of development, this expression pattern for PP2A subunits is consistent with the hypothesis that this phosphatase complex may mediate myosin II filament/monomer cycling during this phase.

Generation and genomic PCR analysis of phr2aBα- and phr2aBβ-null cells. To test for possible roles of phr2aBα and phr2aBβ in myosin II functions *in vivo*, we generated gene disruption lines for each gene. Candidate knockout lines were screened by genomic PCR (Fig. 1 and data not shown). A genomic PCR using a phr2aBα-specific primer set reveals the wild-type (WT) phr2aBα PCR product of 1,296 bp in parental cells, whereas null cells showed a 1,155-bp PCR product due to the replacement insertion of the blasticidin

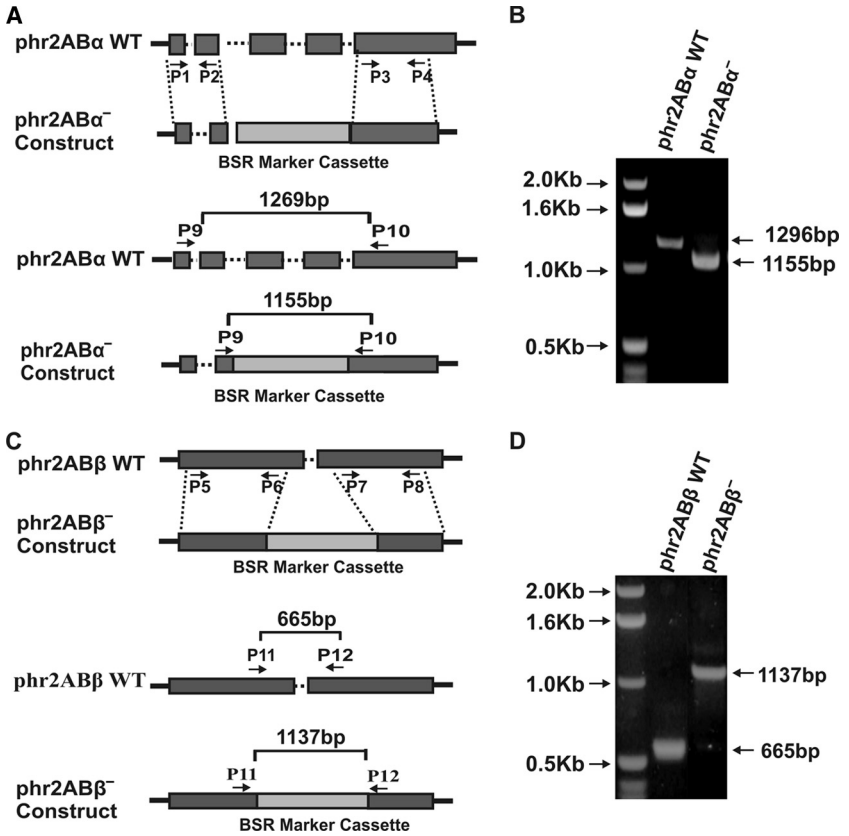

FIG. 1. Generation of phr2aBα and phr2aBβ knockout cell lines and analysis via genomic PCR. (A) The top panel shows a schematic of gene replacement by homologous recombination, indicating the wild-type (WT) phr2aBα locus and the blasticidin-resistant knockout construct that was generated using PCR primers P1 to P4. Exons (boxes) and introns (dotted lines) are indicated. The vertical dotted lines indicate predicted homologous recombination regions. The bottom panel indicates primers used for the PCR screening of the knockout clones. (B) Agarose gel electrophoresis of the genomic PCR screening presenting profiles of parental and phr2aBα knockout products. (C) The top panel shows a schematic of gene replacement by homologous recombination, indicating the wild-type (WT) phr2aBβ locus and the blasticidin-resistant knockout construct that was generated using PCR primers P5 to P8. The vertical dotted lines indicate predicted homologous recombination regions. The bottom panel indicates primers used for the PCR screening of the knockout clones. (D) Agarose gel electrophoresis of the genomic PCR screening presenting profiles of parental and phr2aBβ knockout products.

cassette (Fig. 1B). Similarly, the wild-type parental cells display a phr2aBβ PCR product of 665 bp, whereas phr2aBβ-null cells reveal a 1,137-bp product (Fig. 1D). Western blot analysis of lysates using an anti-phr2aBα antibody revealed an absence of the phr2aBα protein in the phr2aBα-null lines (Fig. 2). Abundance of MHC was not affected in either class of null cells (Fig. 2, top panel). Similarly, abundance of other PP2A subunits was not changed in the knockout lines (Fig. 2). The widely conserved B55 peptide motif LKSLEIEEKINKIR, to which our original phr2aBα antibody was produced (16), is not conserved in the phr2aBβ gene, so antibody-based detection of the phr2aBβ protein product was not possible.

Increased slug formation in null cell lines. Upon nutrient depletion, *Dictyostelium* cells enter a multicellular developmental program leading to the formation of multicellular fruiting bodies and dormant spores. Previous studies showed that myosin II is essential for the morphological changes that accompany development. Gene disruption of *mhcA* results in the reduction of cell migration ability, with development arresting at the mound stage (4, 12). To assess

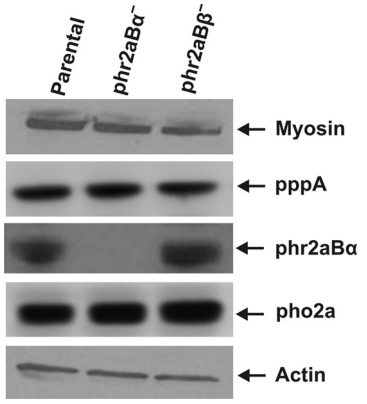

FIG. 2. Western blot analysis of total cell lysates representing the relative abundance of MHC, PP2A scaffolding subunit pppA, PP2A catalytic subunit pho2a, and B55 subunit phr2aBα in parental and knockout cell lines. Total actin levels are presented as a loading control. Presented expression patterns are typical of several independent knockout clones analyzed for each B55 gene (data not shown).

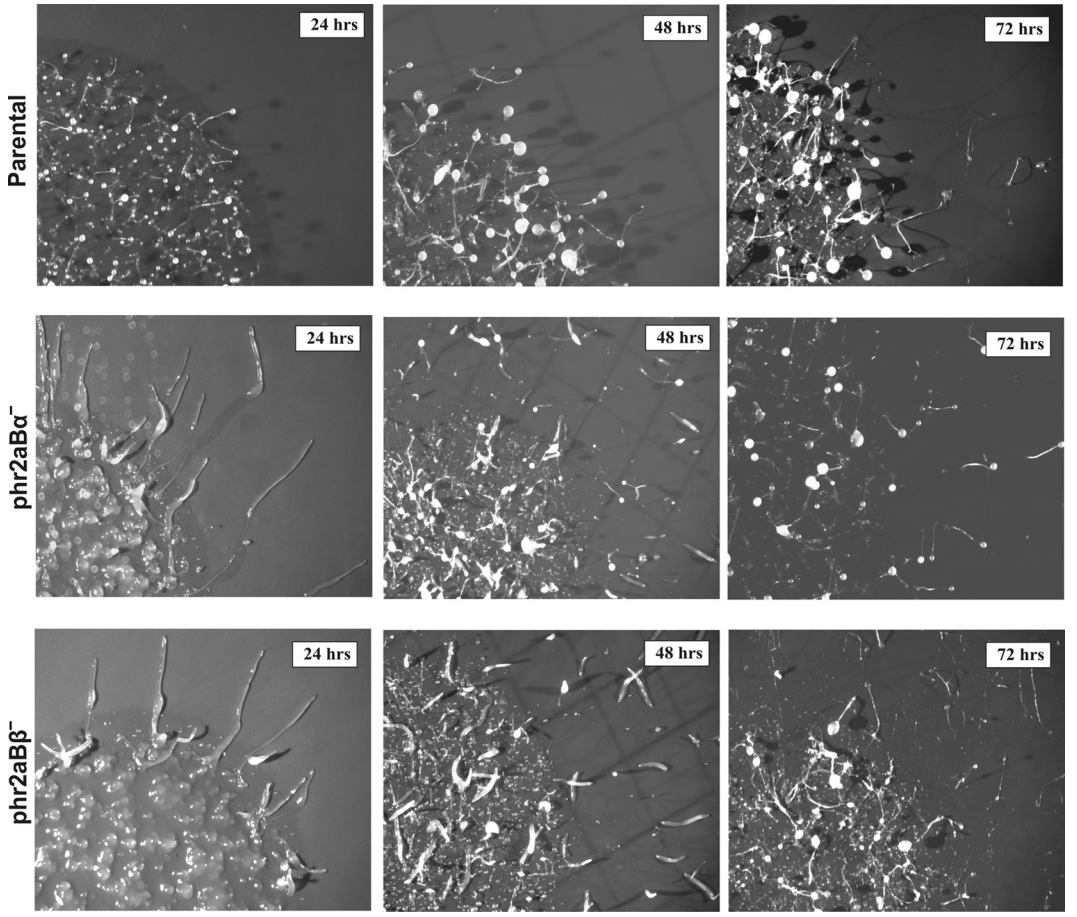

FIG. 3. Developmental delay and increased slug formation in phr2aBα- and phr2aBβ-null cells. For each line, cells were plated in an approximately 15-mm spot on starvation buffer-agar plates and allowed to develop for the indicated amounts of time.

potential roles of phr2aBα and phr2aBβ during the developmental program, null cells were monitored throughout development. Sorocarp formation was delayed in both phr2aBα- and phr2aBβ-null cells by more than 24 h during development. This phenotype was observed in multiple independent clones of each knockout line (Fig. 3 and data not shown). Both classes of knockout lines also displayed an increased propensity to produce migratory slugs during the early phase of development. The reintroduction of FLAG-tagged phr2aBα into either phr2aBα- or phr2aBβ-null cells restored normal developmental timing and reverted the excessive slug formation (Fig. 4). We assessed phototactic ability by plating parental and knockout cells on starvation buffer-agar plates and incubating plates with a unidirectional pinhole light source. On buffered plates in the dark, parental AX2 cells produce few migratory slugs, while both mutant lines produced large numbers of migratory slugs that moved in an appropriate direction via phototaxis (see Fig. S2 in the supplemental material). In addition to producing 4 to 5 times more slugs than parental cells, slugs from both mutant cell lines migrated significantly greater distances during the 48 h of the phototaxis experiment.

B55 involvement in the regulation of myosin II expression and assembly. To test for possible roles of B55 subunits in the regulation of myosin II dephosphorylation and assembly *in vivo*, we quantified myosin II assembly into Triton X-100-resistant cytoskeletal ghosts using previously described methods (5, 13). In previous studies, the functional importance of myosin II tail residues at positions 1823, 1833, and 2029 for filament assembly control was demonstrated by expressing mutated forms of myosin II in *Dictyostelium* myosin II-null cells. In those studies, a triple alanine substitution myosin II construct (3XALA) and a phosphomimetic triple aspartate substitution construct (3XASP) were evaluated for assembly levels with the ghost assay (5). Those cells lines were used as controls for the current analysis. As in the original analysis, the 3XASP construct displayed assembly into cytoskeletal ghosts that is only slightly lower than assembly levels of wild-type myosin II (Fig. 5). However, given previous evidence that 3XASP myosin II cannot support either cytokinesis or multicellular development (5), its association with cytoskeletal ghosts is likely due to trapping of monomers during ghost isolation. As in previous analyses, 3XALA myosin II, blocked for phosphorylation by MHCK A, B, or C, displayed severe overassembly (Fig. 5). Evaluation of the phr2aBα and phr2aBβ cell lines was performed in parallel to ask where either the subunit had critical or detectable roles in targeting the PP2A core dimer to phosphorylated myosin II *in vivo*. This analysis revealed a modest

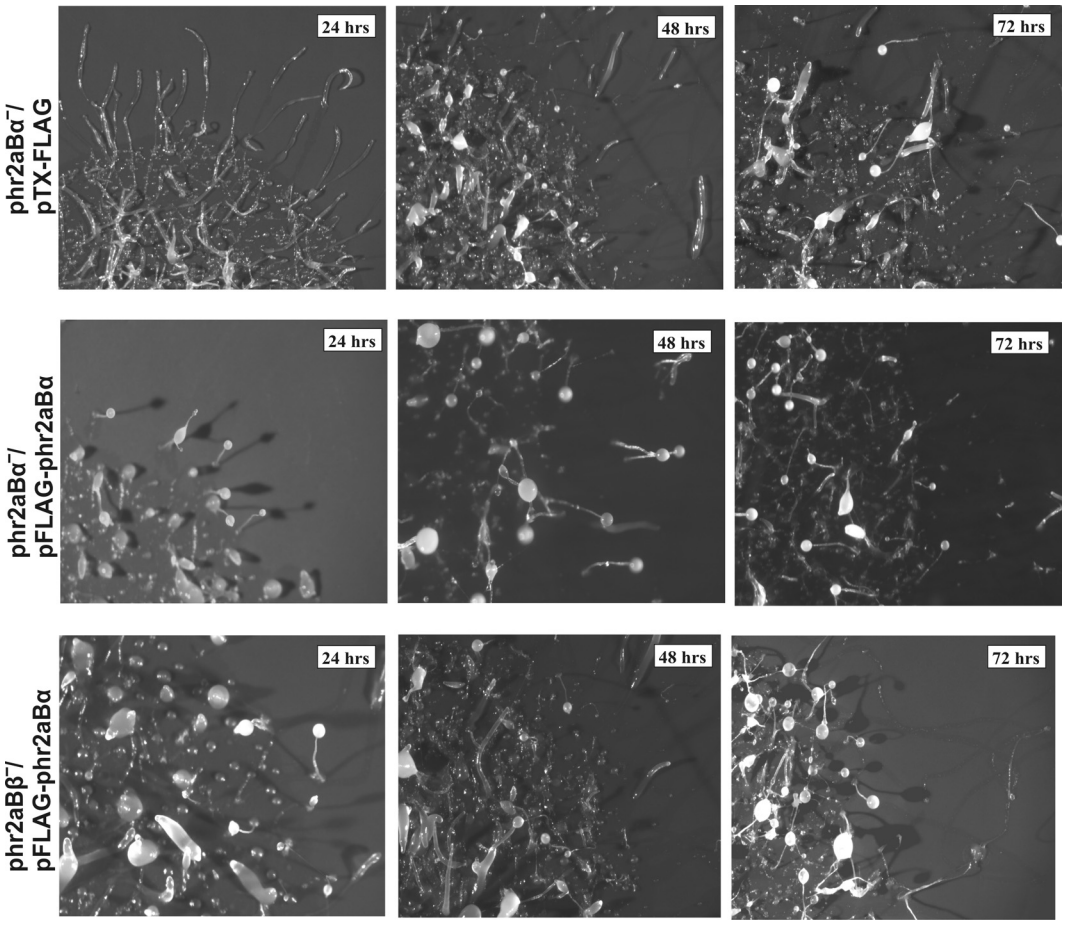

FIG. 4. This developmental delay is rescued in each null cell line (phr2aBα and phr2aBβ) by reintroduction of a FLAG-tagged phr2aBα plasmid construct. Cells were collected and developed on an agar plate as described in legend to Fig. 3, and images were collected at the times indicated.

but statistically significant decrease in myosin II assembly levels in the phr2aBα-null lines and a more modest (and not statistically significant) decrease in myosin II assembly levels in the phr2aBβ-null cells (Fig. 5). Although the decrease in assembly in the phr2aBα appears modest in this analysis, it is noteworthy that assembly levels decrease to a level comparable to that of the 3XASP mutant, consistent with the hypothesis that the phr2aBα does in fact play a role in targeting the PP2A core dimer to cytosolic myosin II filaments to help drive their dephosphorylation and assembly.

B55 regulates myosin II function during cytokinesis. Myosin II is essential for *Dictyostelium* cells to grow in suspension culture, but it is not essential for growth on attached surfaces (4). To test phr2aBα- and phr2aBβ-null lines for cytokinesis defects, cells were assessed for multinucleation when growing on surface cultures versus growing in shaking suspension cultures. No multinucleation was observed in either null cell line when cells were grown on surfaces, the same behavior as that observed for both parental and *mhcA*-null cell lines (Fig. 6). When placed in suspension culture, phr2aBα-null cells displayed a markedly slower growth rate than the parental control AX2 cells, although this defect was not as severe as the growth defect of *mhcA*-null cells (Fig. 7A). In contrast, the phr2aBβ-null lines displayed growth rates in suspension generally similar to those of the parental line (Fig. 7A). To evaluate whether the phr2aBα growth defect correlated with incomplete cytokinesis, cells were collected from suspension cultures, fixed, and stained with DAPI to score for multinucleation. Evaluation of the *mhcA*-null cells as a control revealed many large and multinucleated cells, as described previously (4). Parallel analysis of PP2A knockout lines revealed increased multinucleation in phr2aBα-null cells and in the phr2aBβ-null cell lines (Fig. 7B and C). This analysis further supports the hypothesis that both phr2aBα and phr2aBβ act *in vivo* to facilitate MHC dephosphorylation to allow myosin II filament assembly. However, the modest effect of phr2aBβ disruption on overall suspension growth rates suggests that phr2aBα may have the more central role in this process during cytokinesis. The increase in multinucleation conferred by phr2aBα disruption could be largely reversed by introduction of a FLAG-phr2aBα plasmid expression construct (Fig. 7B and C), further supporting the specificity of this subunit in regulation of cytokinesis, indicating that B55 may be playing a role in myosin-mediated cytokinesis in suspension.

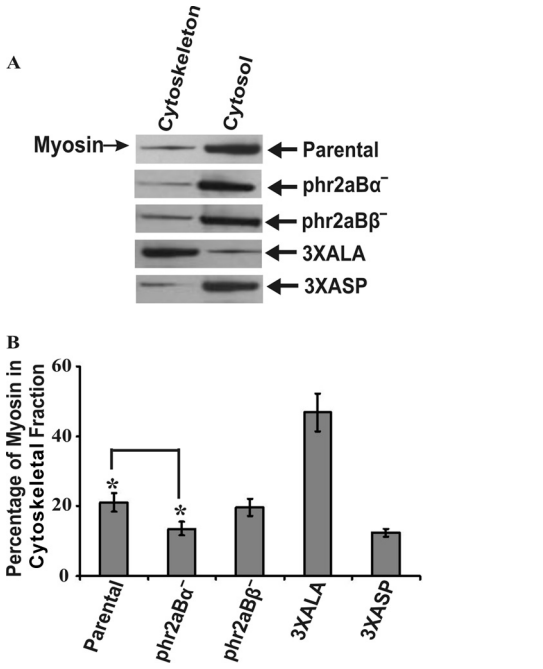

FIG. 5. Quantitation of myosin II assembly in phr2aBα- and phr2aBβ-null cells into Triton-resistant cytoskeletal ghost fractions. (A) Shown are sample SDS-PAGE/Western blot profiles used for quantitative analysis of percentage of myosin II assembled in the Triton-resistant cytoskeletal fractions in parental, 3XALA, 3XASP, and phr2aBα- and phr2aBβ-null cell lines. (B) Quantification of myosin II present in Triton-insoluble fractions in each cell line, determined from densitometry of Western blots. Error bars represent the standard errors of the mean (SEM) with 10 independent samples. *, $P \leq 0.005$.

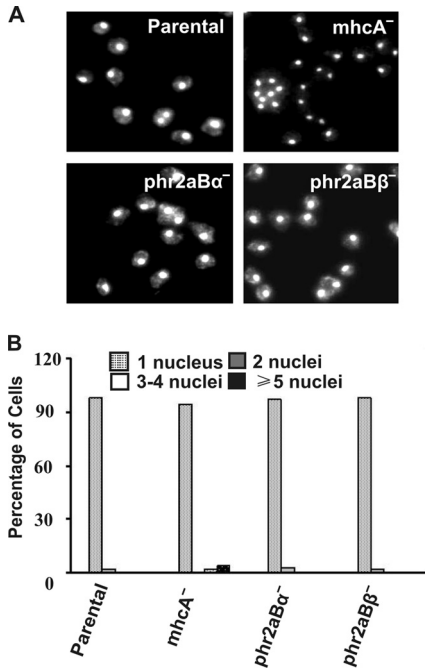

FIG. 6. Quantitation of multinucleation of surface-grown phr2aBα- and phr2aBβ-null cell lines. (A) DAPI staining of cells cultured attached on plastic petri plates for 72 h prior to fixation and staining with DAPI. (B) Bar graph representation of nucleus/cell scored from cells grown on a petri dish. Each graph represents a score of ~200 cells from several fields of view.

DISCUSSION

Although there have been extensive studies in the *Dictyostelium* system, both defining the biochemistry of MHC kinases and validating the *in vivo* importance of the MHC kinases MHCK A, B, and C (13, 20, 23), to date there have been no studies focused on establishing myosin heavy chain protein phosphatase activities in the *in vivo* setting in this system. The work presented here extends the earlier biochemical studies that identified a PP2A trimeric complex as a major MHC phosphatase activity *in vitro* (16). The current work supports the hypothesis that this trimeric complex plays a role in MHC dephosphorylation and filament assembly. However, it is also clear that disruption of either the phr2aBα or the phr2aBβ gene, both putative targeting subunits, does not completely abrogate myosin II filament assembly. This is evident in that multicellular development is delayed but not eliminated, unlike in cells expressing 3XASP mutant myosin or *mhcA*-null cell lines, which completely block development. Interestingly, both phr2aBα and phr2aBβ gene disruption lines also displayed excessive slug formation, phenotypes that could be rescued with expression of FLAG-tagged phr2aBα constructs. Although myosin II is known to be expressed in slugs (6), its roles in slug migration are not well understood. We suggest that the slug phenotype, and possibly the developmental delay, may reflect functions of these B55 targeting subunits that are independent of myosin II.

In contrast, cytoskeletal assembly levels of myosin II, and cytokinesis defects observed in the null lines, fit well with the hypothesis that phr2aBα and phr2aBβ genes produced may influence myosin II assembly levels. However, multiple lines of evidence in the current work suggest that the phr2aBβ gene product has a less significant role in myosin assembly control than does the phr2aBα gene product. First, RNASeq data suggest very low transcript expression levels for this gene during both vegetative growth and development. Second, no defects were observed in the phr2aBβ knockout lines with respect to suspension culture proliferation or with respect to myosin II overassembly into detergent-resistant ghosts. We suggest that PP2A core dimers associated with phr2aBα likely have enhanced activity toward the MHC target sites that regulate filament assembly but that other configurations of PP2A (core dimer, or dimer associated with other B superfamily subunits) probably can also dephosphorylate myosin II heavy chains, accounting for the partial phenotypic defects observed in some assays.

Finally, the identification of a PP2A complex participating *in vivo* in myosin II dephosphorylation and assembly control in *Dictyostelium* parallels the work performed with mast cells, where antigen-induced degranulation and secretion involves regulated myosin II assembly. Holst and colleagues (9) demonstrated that PP2A complexes associated with myosin II and that PP2A inhibition resulted in elevated MHC phosphorylation levels. Collectively, our work and the previous mast cell work argue that PP2A-driven MHC-II dephosphorylation may be a broadly conserved mechanism,

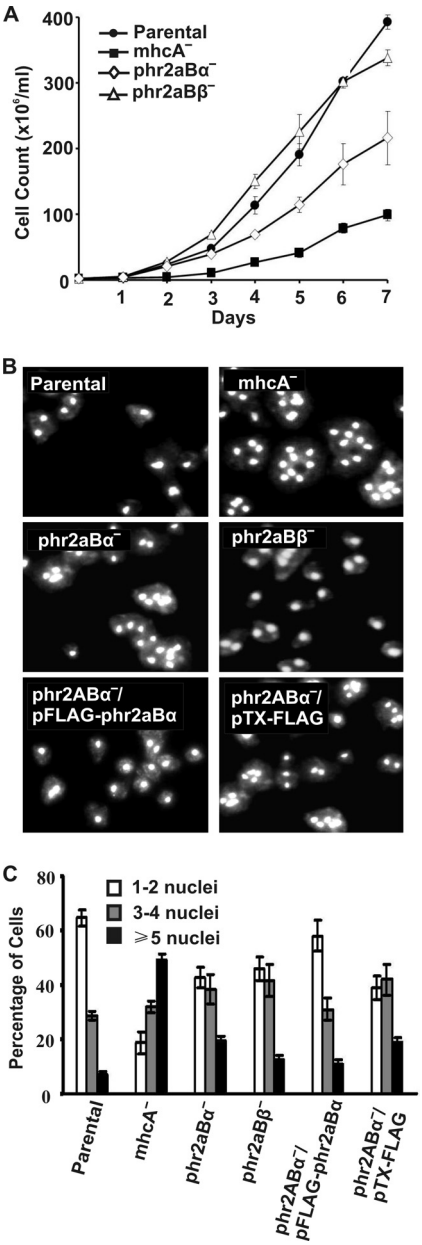

FIG. 7. Growth curves and nuclear staining of phr2aBα- and phr2aBβ-null cell lines grown in suspension. (A) Growth kinetics of parental and *mhcA*-, phr2aBα-, and phr2aBβ-null cell lines in suspension culture. Cells were collected from the petri dish culture and transferred to flasks rotating at 160 rpm in HL5 medium. Cell density was determined by hemocytometer counts every 24 h for 7 days. Data shown are the means and standard errors of five independent experiments. (B) DAPI staining of null cell lines showing multinucleation in suspension culture. For photography, cells were cultured for 72 h in suspension, transferred to glass-bottomed microscope chambers, allowed to attach for 20 min, and then fixed and DAPI stained. (C) Quantitation of multinucleation levels in each cell line scored after 72 h in suspension.

from protista through metazoans, for activating localize myosin II filament assembly.

ACKNOWLEDGMENT

This work was supported by NIH grant GM50009 to T.T.E.

REFERENCES

1. **Berlot, C. H., J. A. Spudich, and P. N. Devreotes.** 1985. Chemoattractant-elicited increases in myosin phosphorylation in Dictyostelium. Cell **43:**307–314.
2. **Betapudi, V., C. Mason, L. Licate, and T. T. Egelhoff.** 2005. Identification and characterization of a novel alpha-kinase with a von Willebrand factor A-like motif localized to the contractile vacuole and Golgi complex in Dictyostelium discoideum. Mol. Biol. Cell **16:**2248–2262. doi:10.1091/mbc.E04-07-0639.
3. **Cho, U. S., and W. Xu.** 2007. Crystal structure of a protein phosphatase 2A heterotrimeric holoenzyme. Nature **445:**53–57.
4. **De Lozanne, A., and J. A. Spudich.** 1987. Disruption of the Dictyostelium myosin heavy chain gene by homologous recombination. Science **236:**1086–1091.
5. **Egelhoff, T. T., R. J. Lee, and J. A. Spudich.** 1993. Dictyostelium myosin heavy chain phosphorylation sites regulate myosin filament assembly and localization in vivo. Cell **75:**363–371.
6. **Eliott, S., P. H. Vardy, and K. L. Williams.** 1991. The distribution of myosin II in Dictyostelium discoideum slug cells. J. Cell Biol. **115:**1267–1274.
7. **Hammer, J. A., III.** 1994. Regulation of Dictyostelium myosin II by phosphorylation: what is essential and what is important? J. Cell Biol. **127:**1779–1782.
8. **Heath, R. J., and R. H. Insall.** 2008. Dictyostelium MEGAPs: F-BAR domain proteins that regulate motility and membrane tubulation in contractile vacuoles. J. Cell Sci. **121:**1054–1064.
9. **Holst, J., A. T. Sim, and R. I. Ludowyke.** 2002. Protein phosphatases 1 and 2A transiently associate with myosin during the peak rate of secretion from mast cells. Mol. Biol. Cell **13:**1083–1098.
10. **Hubbard, M. J., and P. Cohen.** 1993. On target with a new mechanism for the regulation of protein phosphorylation. Trends Biochem. Sci. **18:**172–177.
11. **Janssens, V., and J. Goris.** 2001. Protein phosphatase 2A: a highly regulated family of serine/threonine phosphatases implicated in cell growth and signalling. Biochem. J. **353:**417–439.
12. **Knecht, D. A., and W. F. Loomis.** 1987. Antisense RNA inactivation of myosin heavy chain gene expression in Dictyostelium discoideum. Science **236:**1081–1086.
13. **Kolman, M. F., L. M. Futey, and T. T. Egelhoff.** 1996. Dictyostelium myosin heavy chain kinase A regulates myosin localization during growth and development. J. Cell Biol. **132:**101–109.
14. **Lee, N. S., S. Veeranki, B. Kim, and L. Kim.** 2008. The function of PP2A/B56 in non-metazoan multicellular development. Differentiation **76:**1104–1110.
15. **Mayer-Jaekel, R. E., et al.** 1994. Drosophila mutants in the 55 kDa regulatory subunit of protein phosphatase 2A show strongly reduced ability to dephosphorylate substrates of p34cdc2. J. Cell Sci. **107**(9)**:**2609–2616.
16. **Murphy, M. B., and T. T. Egelhoff.** 1999. Biochemical characterization of a Dictyostelium myosin II heavy-chain phosphatase that promotes filament assembly. Eur. J. Biochem. **264:**582–590.
17. **Murphy, M. B., S. K. Levi, and T. T. Egelhoff.** 1999. Molecular characterization and immunolocalization of Dictyostelium discoideum protein phosphatase 2A. FEBS Lett. **456:**7–12.
18. **Peltz, G., J. A. Spudich, and P. Parham.** 1985. Monoclonal antibodies against seven sites on the head and tail of Dictyostelium myosin. J. Cell Biol. **100:**1016–1023.
19. **Rot, G., et al.** 2009. dictyExpress: a *Dictyostelium discoideum* gene expression database with an explorative data analysis web-based interface. BMC Bioinformatics **10:**265. doi:10.1186/1471-2105-10-265.
20. **Steimle, P. A., T. Naismith, L. Licate, and T. T. Egelhoff.** 2001. WD repeat domains target dictyostelium myosin heavy chain kinases by binding directly to myosin filaments. J. Biol. Chem. **276:**6853–6860.
21. **Xu, Y., et al.** 2006. Structure of the protein phosphatase 2A holoenzyme. Cell **127:**1239–1251.
22. **Yumura, S.** 2001. Myosin II dynamics and cortical flow during contractile ring formation in Dictyostelium cells. J. Cell Biol. **154:**137–146.
23. **Yumura, S., et al.** 2005. Multiple myosin II heavy chain kinases: roles in filament assembly control and proper cytokinesis in Dictyostelium. Mol. Biol. Cell **16:**4256–4266.